

Suzaku observations of Fe K-shell lines in the supernova remnant W51C and hard X-ray sources in the proximity

Kumiko K. Nobukawa^{a,*}

^a*Faculty of Science and Engineering, Kindai University,
3-4-1 Kowakae, Higashi-Osaka, 577-8502, Japan*

E-mail: kumiko@phys.kindai.ac.jp

We have investigated the Fe K-shell lines in W51C with Suzaku, which has the largest effective area in the Fe K-shell band in contemporary X-ray astronomy satellites. The observed 6.7 keV line intensity in the W51C region is consistent with that of the background emission. On the other hand, the observed 6.4 keV line intensity is higher than that of the background with a significance level of 2.0σ . The most likely origin of the enhancement is the interaction between low-energy CRs and molecular clouds. The local enhancement of the 6.7 keV line in the compact H II region G49.0–0.3 was found for the first time with a significance level of 3.4σ . Spectral analysis revealed that the temperature of the thermal plasma accompanied by the Fe line is $kT = 3.0^{+0.8}_{-0.7}$ keV, which could be explained by a thermal plasma produced by the stellar winds of O stars.

*Multifrequency Behaviour of High Energy Cosmic Sources XIV (MULTIF2023)
12-17 June 2023
Palermo, Italy*

*Speaker

1. Introduction

A diffuse X-ray emission along the Galactic plane, that is the Galactic diffuse X-ray emission, was first reported by Worrall et al. (1982) [1] with HEAO-1 observations. They proposed that the most probable origin of the diffuse X-ray emission is an integration of many unresolved faint sources. The Tenma satellite discovered an intense Fe $K\alpha$ emission line at ~ 6.7 keV, which is consistent with the centroid of a He-like Fe $K\alpha$ line, and thus the diffuse emission would come from an optically thin thermal plasma (Koyama et al. 1986 [2]). ASCA resolved the Fe K-shell line from the diffuse X-ray emission into three lines; a neutral Fe line at 6.4 keV, a He-like Fe line at 6.7 keV, and a H-like Fe line at 6.9 keV (Koyama et al. 1996 [3]). The neutral Fe line is produced by photoionization or inner shell ionization of cold gas while the He-like and H-like Fe lines are radiated from a highly ionized plasma with the electron temperature of \gtrsim several keV. Since the three Fe lines are radiated from the matter with different temperatures by the different physical processes, the origin of each of the Fe lines should be discussed separately.

Although it has been under debate whether the origin of the Galactic diffuse X-ray emission is truly diffuse X-ray emission or the integration of many faint point sources, the He-like Fe line at 6.7 keV and the neutral Fe line at 6.4 keV are often observed as the truly diffuse emission. An example of the 6.7 keV line from diffuse emission is plasma in supernova remnants (SNRs). The 6.7 keV line can be emitted at the intensity detectable by X-ray CCDs if the electron temperature of the plasma is $\gtrsim 1$ keV and Fe atoms are highly ionized (c.f. Yamaguchi et al. 2014 [4]). Interestingly, some SNR plasmas emitting the 6.7 keV line are overionized (IC443, W49B, Sgr A East, N132D; Kawasaki et al. 2002 [5], Ozawa et al. 2009 [6], Ono et al. 2019 [7], Bamba et al. 2018 [8]). Another example is star-forming regions (e.g. Ezoe et al. 2006 [9]). The electron temperature kT of shocked stellar winds with the velocity v behind the shock is described by,

$$kT = \frac{3}{16} \mu m_{\text{H}} v^2 = 5 \text{ keV} \left(\frac{v}{2000 \text{ km s}^{-1}} \right)^2. \quad (1)$$

Here, μ and m_{H} are the mean molecular weight and the mass of a hydrogen atom, respectively. OB stars usually show wind velocities in the range of 1000–3000 km s⁻¹ (Prinja 1990 [10]), and thus the temperature can be $\gtrsim 1$ keV, which results in the 6.7 keV line.

As for the 6.4 keV line from diffuse emission, X-ray reflection nebulae (XRNe) in the Galactic center region would be the most famous example (Sunyaev et al. 1993 [11]; Koyama et al. 1996 [3]). Photoionization of Fe atoms in molecular clouds (MCs) occurs by the irradiation of X-ray flares from the supermassive black hole Sagittarius (Sgr) A*. We note that only X-rays with the energy above Fe K-shell edge (~ 7.1 keV) can cause photoionization to produce the 6.4 keV line. The flux of the 6.4 keV line $F_{6.4 \text{ keV}}$ is described by the equation of

$$F_{6.4 \text{ keV}} = \epsilon \left(\frac{\Omega}{4\pi} \right) \int_{7.1 \text{ keV}}^{\infty} (1 - e^{-N_{\text{H}} Z_{\text{Fe}} \sigma_{\text{X}}(E)}) f_{\text{X}}(E) dE, \quad (2)$$

where ϵ , Ω , N_{H} , Z_{Fe} , σ_{X} , and $f_{\text{X}}(E)$ are the fluorescent yield of Fe atoms (0.34; Bambynek et al. 1972 [12]), the solid angle with which the MC is seen from Sgr A*, the hydrogen column density, the Fe abundance (3×10^{-5} , Lodders 2003 [13]), the photoionization cross section of Fe atoms ($6 \times 10^{-18} (E/1\text{keV})^{-2.6} \text{ cm}^2$; Henke et al. 1982 [14]), and the X-ray spectrum of Sgr A*, respectively.

Recently, several studies demonstrated that the 6.4 keV line emission is a probe of low-energy cosmic rays (CRs): MeV protons or keV electrons (c.f. Tatischeff 2003 [15]). CRs intrude into MCs and ionize inner-shell electrons of Fe atoms, and then the 6.4 keV line is produced (c.f. Fujita et al. 2021 [16]). The intensity of the particle-induced 6.4 keV line $I_{6.4 \text{ keV}}$ is described as follows:

$$I_{6.4 \text{ keV}} = \frac{1}{4\pi} N_{\text{H}} \int \sigma_{6.4 \text{ keV}}(E) v(E) f_{\text{CR}}(E) dE. \quad (3)$$

Here, $\sigma_{6.4 \text{ keV}}(E)$, $v(E)$, and $f_{\text{CR}}(E)$ are the cross section of production of the 6.4 keV line via inner-shell ionization of Fe atoms (see Tatischeff 2003 [15]), particle velocity, and the particle spectrum, respectively. Nobukawa et al. (2015) [17] discovered the enhancement of the 6.4 keV line near the Bania's clump in the Galactic center ($l \sim 3^\circ$; Bania 1977 [18]) and found that its most plausible origin is bombardments of low-energy CR proton. Also, the low-energy CRs would contribute to at least a part of the 6.4 keV line emission from the Galactic diffuse X-ray emission (Yamauchi et al. 2016 [19]; Nobukawa et al. 2016 [20]). SNRs, one of the most promising candidates for CR acceleration, can emit the 6.4 keV line. In fact, more than 10 SNRs show the 6.4 keV line, which cannot be explained by the photoionization and is most likely of the CR origin (e.g., Kes 79, W28, W44, and IC443; Sato et al. 2016 [21], Nobukawa et al. 2018 [22], 2019 [23]).

The effective area of detectors is important to observe the Fe K-shell line of faint diffuse emission. Among the contemporary X-ray astronomy satellites (Chandra, XMM-Newton, Suzaku, NuSTAR, eROSITA and XRISM), NuSTAR and Suzaku have the largest effective area ($\sim 800\text{--}900 \text{ cm}^2$) in the Fe K-shell band (see Predehl et al. 2021 [24] and XRISM Quick Reference [25]). But NuSTAR cannot resolve the Fe-K line into the 6.4 keV and 6.7 keV lines. Although Suzaku has been out of operation since 2016, it is still the best instrument for observing the Fe K-shell line of faint diffuse emission. In fact, many of the above-mentioned results on the 6.4 keV and 6.7 keV lines from the diffuse emission were accomplished by Suzaku.

In this study, we focus on the middle-aged and mixed morphology supernova remnant W51C observed in the Fe K-shell band. W51C is superposed on the massive star-forming region W51B, which contains several compact H II regions. MC-SNR interaction in W51C is indicated by OH masers (Green et al. 1997 [26]). W51C is also thought to be a CR accelerator. Gamma-rays probably produced by π^0 decay were found in the SNR (Abdo et al. 2009 [27]; Fiasson et al. 2009 [28]; Aleksić et al. 2012 [29]), and the GeV gamma-ray luminosity is $1 \times 10^{36} (D/6 \text{ kpc})^2 \text{ erg s}^{-1}$ in the 0.2–50 GeV band ((Abdo et al. 2009 [27]), which makes the SNR one of the most luminous Galactic sources in gamma-rays. The high ionization rate of $\zeta \sim 10^{-15} \text{ s}^{-1}$ was obtained by a measurement of the $[\text{DCO}^+]/[\text{HCO}^+]$ abundance ratio via millimeter wave spectroscopy (Ceccarelli et al. 2011 [30]), which implies the existence of a large number of low-energy CRs in the vicinity of W51C. Previous X-ray observations of W51C revealed that there are several bright point/extended sources in the proximity; the pulsar wind nebular (PWN) candidate CXO J192318.5+140305 (Koo et al. 2005 [31]), another PWN candidate HX3west (Koo et al. 2002 [32]; Sasaki et al. 2014 [33]), and a few extended emissions possibly corresponding to compact H II regions (G48.9–0.3, G49.0–0.3, and G49.2–0.3). We analyzed the Suzaku data of W51C and reported the result in Shimaguchi et al. (2022) [34]. This paper summarizes the highlights of our results and reports on prospects for the low-energy CR study via the neutral Fe line observations. Errors quoted in this paper and error bars given in the figures show 1σ statistical errors.

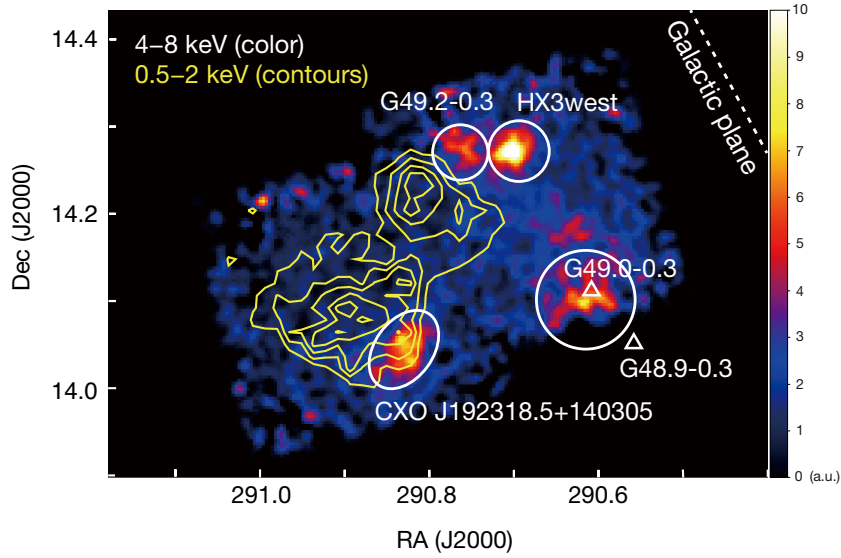


Figure 1: Hard X-ray image of W51C obtained by Suzaku in the 4–8 keV band (color) overlaid by the soft band (0.5–2 keV) image (contours). Circles and ellipses are the hard X-ray sources, CXO J192318.5+140305, HX3west, H II regions G49.2–0.3 and G49.0–0.3.

2. Suzaku observation of W51C and results

2.1 Observations

We analyzed the Suzaku archive data of two observations of W51C (OBSID: 504066010 and 504067010). The observations were conducted on March 28–31, 2010. We used the data of the X-ray Imaging Spectrometer (XIS; Koyama et al. 2007 [35]), which consists of four X-ray CCD cameras (XIS 0, 1, 2, and 3). The whole region of XIS 2 and a quarter of XIS 0 have been out of use since 2006 November and 2009 June, respectively; hence the data from these regions were not used. The field of view (FOV) of each CCD is $17'.8 \times 17'.8$.

Figure 1 shows a hard X-ray image obtained by Suzaku in the 4–8 keV band (color) overlaid by the soft band image (0.5–2 keV; yellow contours). The images of XIS 0, 1, and 3 were merged. The non X-ray background estimated by `xisnxbgen` (Tawa et al. 2008 [36]) was subtracted, and the vignetting was corrected. The hard X-ray objects previously reported, CXO J192318.5+140305, HX3west, H II regions G49.2–0.3 and G49.0–0.3 are seen in the image. The H II region G48.9–0.3 is out of the FOV.

2.2 Fe line measurement

The size of the radio shell of W51C is $\sim 40'$ (Stil et al. 2006 [37]; Beuther et al. 2016 [38]), and it covers the whole FOVs. Since CR acceleration occurs in the shell, the 6.4 keV line can be emitted in the whole FOVs. We extracted a spectrum from the whole FOVs using the XIS 0, 1, and 3 data. The regions including the four hard X-ray objects (the circles and ellipses in figure 1) were excluded. The spectrum is shown in figure 2. We clearly see the neutral Fe $K\alpha$ at 6.4 keV, the He-like Fe $K\alpha$ at 6.7 keV, and the H-like Fe $K\alpha$ at 6.9 keV. W51C is located near the Galactic plane (see figure 1), and therefore the Fe K-shell lines come from the Galactic diffuse X-ray emission and also possibly from W51C. We fitted the spectrum of the high-energy band above 4.5 keV to avoid contamination by local soft X-ray emission from W 51 C (cf. Hanabata et al. 2013 [39]; Sasaki et al. 2014 [33]). The fitted model was an absorbed thermal bremsstrahlung plus four Gaussians in addition to the cosmic X-ray background (CXB), that is `phabs*(bremsstrahlung +`

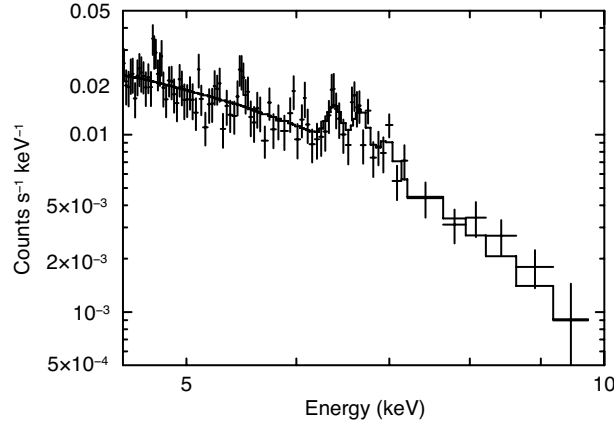


Figure 2: Spectra of the whole W51C region in the 4.5–10 keV band.

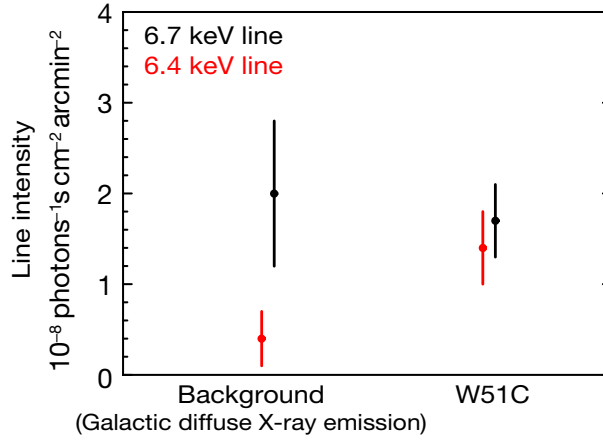


Figure 3: Comparison of line intensities of 6.4 keV and 6.7 keV lines between the background (the Galactic diffuse X-ray background) and the W51C region (the whole FOVs).

gaussian + gaussian + gaussian + gaussian) in XSPEC. The four Gaussians represent the Fe K-shell lines, and the centroids were fixed to 6.40 and 7.05 keV (the neutral Fe $K\alpha$ and $K\beta$), 6.68 keV (He-like Fe $K\alpha$), and 6.97 keV (H-like Fe $K\alpha$). The normalization of the neutral Fe $K\beta$ was fixed to 0.125 times that of the $K\alpha$ (Kaastra & Mewe 1993 [40]; Smith et al. 2001 [41]). The parameters of the CXB were fixed to the values in Kushino et al. (2002) [42]. Figure 3 shows the obtained intensities of the 6.4 and 6.7 keV lines, which are $(1.4 \pm 0.4) \times 10^{-8}$ and $(1.7 \pm 0.4) \times 10^{-8}$ in units of photons $s^{-1} \text{ cm}^{-2} \text{ arcmin}^{-2}$, respectively.

Since the radio shell of W51C covers the whole Suzaku FOVs, no data can be used as background regions in the same FOVs. We estimated the intensities of the Fe K-shell lines of the background, based on the Galactic diffuse X-ray background model of previous studies. The distributions of the 6.4 and 6.7 keV lines along the Galactic plane were well studied by Uchiyama et al. (2013) [43] and Yamauchi et al. (2016) [19]. Using the scale lengths and scale heights of the Fe lines obtained by the previous studies, we estimated the line intensities at the central coordinate of the W51C regions ($l = 49^\circ.11$, $b = -0^\circ.43$) to be $(0.4 \pm 0.3) \times 10^{-8}$ and $(2.0 \pm 0.8) \times 10^{-8}$ in units of photons $s^{-1} \text{ cm}^{-2} \text{ arcmin}^{-2}$ for the 6.4 and 6.7 keV lines, respectively, which are indicated as the “Background” data in figure 3. The observed intensity of the 6.7 keV line (the “W51C” black data in figure 3), $(1.7 \pm 0.4) \times 10^{-8}$ photons $s^{-1} \text{ cm}^{-2} \text{ arcmin}^{-2}$, is

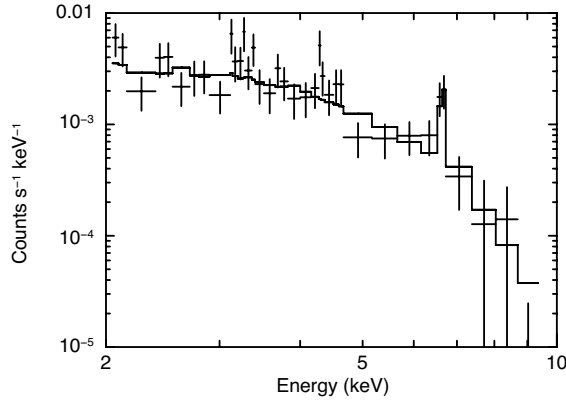


Figure 4: Background-subtracted spectrum of G49.0–0.3. The solid black line represents the best-fit model (see text).

consistent with the background. But the observed intensity of the 6.4 keV line (the “W51C” red data in figure 3), $(1.4 \pm 0.4) \times 10^{-8} \text{ cm}^{-2} \text{ arcmin}^{-2}$, is higher than the background at a significance level of 2.0σ . This indicates a hint of an enhancement in the 6.4 keV line emission in the W51C region.

2.3 Hard X-ray sources in the proximity

Another highlight of Shimaguchi et al. 2022 [34] is the discovery of the 6.7 keV line from the H II region G49.0–0.3. The 6.7 keV line intensity in the W51C is almost constant over the W51C region within the error ranges, but the exception is G49.0–0.3, where the line intensity is $(9.9 \pm 2.4) \times 10^{-8} \text{ photons s}^{-1} \text{ cm}^{-2} \text{ arcmin}^{-2}$, higher than the average of the W51C region ($(1.7 \pm 0.4) \times 10^{-8} \text{ photons s}^{-1} \text{ cm}^{-2} \text{ arcmin}^{-2}$) at a significance level of 3.4σ . The spectrum shown in figure 4 clearly represents the 6.7 keV line. The enhancement of the thermal Fe K-shell line emission implies the presence of high-temperature plasma. We fitted the G49.0–0.3 spectrum in the 2–10 keV band with an absorbed collisional ionization equilibrium (CIE) plasma model (phabs×apec in XSPEC). A background spectrum was extracted from the surrounding region to take into account not only the W51C contamination but also the contribution of the hard X-ray emission in the W51B region (Hanabata et al. 2013 [39]). The best-fit hydrogen column density, temperature and abundance of the CIE plasma were obtained to be $N_{\text{H}} = 2.5^{+1.2}_{-0.9} \times 10^{22} \text{ cm}^{-2}$, $kT = 3.0^{+0.8}_{-0.7} \text{ keV}$ and 0.5 ± 0.2 solar, respectively, The reduced χ^2 value was 1.12 (d.o.f. = 52). The flux of the 2–10 keV band was obtained to be $3.7 \times 10^{-13} \text{ erg s}^{-1} \text{ cm}^{-2}$.

3. Discussion

3.1 Origin of the enhancement of the 6.4 keV line in the W51C region

We found the enhancement of the 6.4 keV line at a significance level of 2.0σ in the W51C region. Although this is not a robust result, here we discuss the possible origins of the enhancement, assuming that it is real.

One possible scenario is the K-shell line from low-ionized Fe in an SNR plasma with the non-equilibrium ionization (NEI) state. The observed 6.4 keV line has the upper limit of the centroid of 6.430 keV, which corresponds to the ionization state of Ne-like Fe and the ionization time-scale of $\sim 200 \text{ yr}$ according to code in XSPEC (if $n_e=1 \text{ cm}^{-3}$). This is two orders of magnitudes younger than the age of W51C ($3 \times 10^4 \text{ yr}$; Koo et al. 1995 [44]). Thus we rejected the plasma origin and concluded that the 6.4 keV line comes from the neutral Fe atoms.

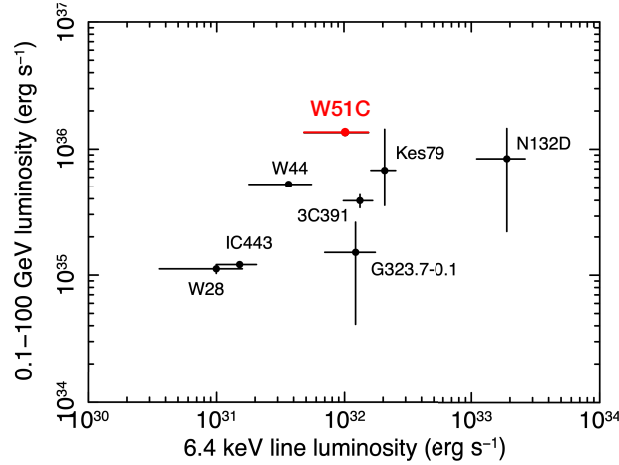


Figure 5: Comparison between the 6.4 keV line luminosity and 0.1–100 GeV gamma-ray luminosity for W51C and previous studies (from Shimaguchi et al. 2022 [34]).

Photoionization and low-energy CR bombardment are the possible origins. The intensity of the 6.4 keV line in the photoionization scenario is estimated by equation (2). We assume $A(E) = K(E/1\text{keV})^{-\Gamma}$ as the X-ray spectrum of the irradiating X-ray source with the photon index Γ and normalization K . Candidates for the irradiating sources are the four hard X-ray sources near W51C, and their photon index Γ ranges from 1.8–3.2 (Sasaki et al. 2014 [33]; Shimaguchi et al. 2022 [34]). Adopting the upper limits of the hydrogen column densities $N_{\text{H}} \geq 1.8 \times 10^{21} \text{ cm}^{-2}$ (Koo et al. 1997 [45]), we estimated the required flux of the external X-ray source to be $(0.07\text{--}1) \times 10^{-8} \text{ erg s}^{-1} \text{ cm}^{-2}$ in the 0.3–10 keV band. This is at least two orders of magnitude higher than the flux of the hard X-ray sources, regardless of the solid angle, and hence we rejected the photoionization origin.

The low-energy CRs bombardment is the most plausible origin. The particle-induced 6.4 keV line intensity is expressed by equation (3). Assuming CR protons with the monoenergetic distribution of 10 MeV, we estimated the energy density to be $\sim 150 \text{ eV cm}^{-3}$. If the 6.4 keV line originates from low-energy protons interacting with MCs, we can expect a positive correlation between the luminosities of the 6.4 keV line and gamma-rays. Shimaguchi et al. 2022 [34] reported that there is a hint of a positive correlation between the two observables (the correlation coefficient is $r \sim 0.3$; figure 5) although the sample size is limited.

3.2 Origin of the enhancement of the 6.7 keV line in G49.0–0.3

We found the enhancement of the 6.7 keV line in the H II region G49.0–0.3. The wind temperature behind the stellar shock is expressed by equation (1). The observed temperature of the G49.0–0.3 spectrum is $kT = 3.0_{-0.7}^{+0.8} \text{ keV}$, which corresponds to the wind velocity of $v \sim 1500 \text{ km s}^{-1}$. The most massive star in G49.0–0.3 is an O9 star (Kim et al. 2007 [46]), and the typical wind velocity of O stars is 1000–3000 km s^{-1} (Prinja 1990 [10]). The observed abundance 0.5 ± 0.3 solar is consistent with values in other H II regions (e.g., Hyodo et al. 2008 [47]). Therefore, the enhancement of the 6.7 keV line would be due to the high-temperature plasma associated with the H II region.

3.3 Prospects

On September 7, 2023, the XRISM satellite, which has been developed under an international collaboration of JAXA, NASA, and ESA, was successfully launched. XRISM is equipped with the micro-calorimeter Resolve with a high energy resolution of $\sim 5 \text{ eV}$ in the Fe K-shell band. The FOV of Resolve is narrow (3

arcmin sq.), generally making it unsuitable for observing diffuse emissions. Nevertheless, for bright SNRs, Resolve has the potential to detect the 6.4 keV line thanks to its high energy resolution, and XRISM is expected to accelerate the study of low-energy CRs.

DISCUSSION

Dr. Jordan Eagle: Many researchers use the Fe $K\alpha$ (6.4 keV) to interpret Type Ia or CC SNe (prominent Fe $K\alpha$ often shown to be in Type Ia, but you nicely showed a variety of SNRs both CC + Type Ia that have no 6.7 keV but have 6.4 keV and you interpret this nicely as potential signature for CR acceleration, which applies to both types of SNRs. Notably, you clarify a focus on overionized systems what was interesting implications for the conditions any SNR needs to possess to accelerate efficiently.

Author: All our sample SNRs have low-temperature plasma with $kT < 1$ keV, where no detectable Fe K-shell line at CCD energy resolution would be found regardless of the centroids (neither 6.4 keV nor 6.7 keV would be found). Therefore, we could easily find the particle-induced Fe line. However, this is not the case when investigating an SNR plasma with an electron temperature above 1 keV; the Fe line at ~ 6.4 keV can be of the ejecta origin.

Interestingly, not a few parts of SNRs that show the possible particle-induced Fe line have overionized plasma. At present, we do not know whether it may be because the conditions under which SNR plasma becomes overionized are similar to those under which (low-energy) CRs are efficiently accelerated, or it implies that low-energy CRs contribute to overionizing plasma. I would like to investigate this point in more detail.

Acknowledgments

The author is most grateful to the organizers for their kind invitation to give this talk at this fantastic workshop. The author wishes to acknowledge my collaborators: Dr. Shigeo Yamauchi, Dr. Masayoshi Nobukawa, Dr. Yutaka Fujita, and also a bright graduate student, Aika Shimaguchi. This research is supported by MEXT KAKENHI No. JP20K14491, JP20KK0071, 23H00151 (KN), JP21K03615 (MN), JP18K03647, and JP20H00181 (YF). KKN is also supported by the Yamada Science Foundation and the Mitsubishi Foundation.

References

- [1] D. M. Worrall et al. *HEAO 1 Measurements of the Galactic Ridge*, *ApJ* **255** 111–121
- [2] K. Koyama et al. *Thermal X-Ray-Emission with Intense 6.7-keV Iron Line From the Galactic Ridge* *PASJ* **38** 121–131
- [3] K. Koyama et al. *ASCA View of Our Galactic Center: Remains of Past Activities in X-Rays?* *PASJ* **48** 249–255
- [4] H. Yamaguchi et al. *Discriminating the Progenitor Type of Supernova Remnants with Iron K-shell Emission* *ApJL* **785** L27
- [5] M. Kawasaki et al. *ASCA Observations of the Supernova Remnant IC 443: Thermal Structure and Detection of Overionized Plasma* *ApJ* **572** 897–905
- [6] M. Ozawa et al. *Suzaku Discovery of the Strong Radiative Recombination Continuum of Iron from the Supernova Remnant W49B* *ApJL* **706** L71–L75

- [7] A. Ono et al. *X-ray spectra of Sagittarius A East and diffuse X-ray background near the Galactic center* *PASJ* **71** 52
- [8] A. Bamba et al. *The Transition from Young to Middle-aged Supernova Remnants: Thermal and Nonthermal Aspects of SNR N132D* *ApJ* **854** 71
- [9] Y. Ezoe et al. *Investigation of Diffuse Hard X-Ray Emission from the Massive Star-forming Region NGC 6334*, *ApJ* **638** 860–877
- [10] R. K. Prinja et al. *Similarities in the wind characteristics of hot stars*, *A&A* **232** 119–125
- [11] R. A. Sunyaev et al. *The Center of the Galaxy in the Recent Past - a View From Granat*, *ApJ* **407** 606–610
- [12] W. Bambynek et al. *X-Ray Fluorescence Yields, Auger, and Coster-Kronig Transition Probabilities*, *Rev. Mod. Phys.* **44** 716
- [13] K. Lodders et al. *Solar System Abundances and Condensation Temperatures of the Elements*, *ApJ* **591** 1220–1247
- [14] B. L. Henke et al. *Low-Energy X-Ray Interaction Coefficients: Photoabsorption, Scattering, and Reflection, $E=100\text{--}2000$ eV, $Z=1\text{--}94$* , *At. Data Nucl. Data Tables* **27** 1–144
- [15] V. Tatischeff et al. *X- and Gamma-Ray Line Emission Processes*, *EAS Publications Series* **7** 79
- [16] Y. Fujita et al. *Intrusion of MeV–TeV Cosmic Rays into Molecular Clouds Studied by Ionization, the Neutral Iron Line, and Gamma Rays*, *ApJ* **908** 136
- [17] K. K. Nobukawa et al. *Enhancement of the 6.4 keV Line in the Inner Galactic Ridge: Proton-induced Fluorescence?*, *ApJL* **807** L10
- [18] T. M. Bania *Carbon monoxide in the inner Galaxy*, *ApJ* **216** 381–403
- [19] S. Yamauchi et al. *Scale heights and equivalent widths of the iron K-shell lines in the Galactic diffuse X-ray emission*, *PASJ* **68** 59
- [20] M. Nobukawa et al. *Origin of the Galactic Diffuse X-Ray Emission: Iron K-shell Line Diagnostics*, *ApJ* **833** 268
- [21] T. Sato et al. *Suzaku spectra of a Type-II supernova remnant, Kes 79*, *PASJ* **68** S8
- [22] K. K. Nobukawa et al. *Evidence for a Neutral Iron Line Generated by MeV Protons from Supernova Remnants Interacting with Molecular Clouds*, *ApJ* **854** 87
- [23] K. K. Nobukawa et al. *Neutral iron line in the supernova remnant IC 443 and implications for MeV cosmic rays*, *PASJ* **71** 115
- [24] P. Predehl et al. *The eROSITA X-ray telescope on SRG*, *A&A* **647** A1
- [25] XRISM science team, *XRISM Quick Reference*, arXiv:2202.05399
- [26] A. J. Green et al. *Continuation of a survey of OH (1720 MHz) Maser Emission Towards Supernova Remnants*, *ApJ* **14** 2058

- [27] A. A. Abdo et al. *Fermi LAT Discovery of Extended Gamma-Ray Emission in the Direction of Supernova Remnant W51C*, *ApJL* **706** L1–L6
- [28] A. Fiasson et al. *Discovery of a VHE gamma-ray source in the W51 region*, *Proceedings of the st ICRC*
- [29] J. Aleksić et al. *Morphological and spectral properties of the W51 region measured with the MAGIC telescopes.*, *A&A* **541** A13
- [30] C. Ceccarelli et al. *Supernova-enhanced Cosmic-Ray Ionization and Induced Chemistry in a Molecular Cloud of W51C*, *ApJL* **740** L4
- [31] B.-C. Koo et al. *Chandra Observations of the W51C Supernova Remnant*, *ApJ* **633** 946–952
- [32] B.-C. Koo et al. *An ASCA Study of the W51 Complex*, *ApJ* **123** 1629–1638
- [33] M. Sasaki et al. *XMM-Newton observation of the Galactic supernova remnant W51C (G49.1–0.1)*, *A&A* **563** A9
- [34] A. Shimaguchi et al. *Suzaku observations of Fe K-shell lines in the supernova remnant W 51 C and hard X-ray sources in the proximity*, *PASJ* **74** 656–663
- [35] K. Koyama et al. *X-ray Imaging Spectrometer (XIS) on board Suzaku*, *PASJ* **59** S23–S33
- [36] N. Tawa et al. *Reproducibility of Non-X-Ray Background for the X-Ray Imaging Spectrometer aboard Suzaku*, *PASJ* **60** S11–S24
- [37] J. M. Stil et al. *The VLA Galactic Plane Survey*, *AJ* **132** 1158–1176
- [38] H. Beuther et al. *The HI/OH/Recombination line survey of the inner Milky Way (THOR)*, *A&A* **595** A32
- [39] Y. Hanabata et al. *X-Ray Observations of the W51 Complex with Suzaku*, *PASJ* **65** 42
- [40] J. S. Kaastra & R. Mewe *X-ray emission from thin plasmas. I - Multiple Auger ionisation and fluorescence processes for Be to Zn*, *A&A Supplement Series* **97** 443–482
- [41] R. K. Smith et al. *Collisional Plasma Models with APEC/APED: Emission-Line Diagnostics of Hydrogen-like and Helium-like Ions*, *ApJL* **556** L91–L95
- [42] A. Kushino et al. *Study of the X-ray background spectrum and its large-scale fluctuation with ASCA*, *PASJ* **54** 327–352
- [43] H. Uchiyama et al. *K-Shell Line Distribution of Heavy Elements along the Galactic Plane Observed with Suzaku*, *PASJ* **65** 19
- [44] B.-C. Koo et al. *ROSAT Observations of the Supernova Remnant W51C*, *ApJ* **447** 211
- [45] B.-C. Koo & D.-S. Moon *Interaction between the W51C Supernova Remnant and a Molecular Cloud. I. HI 21 Centimeter Line Observations*, *ApJ* **475** 194–210
- [46] H.-S. Kim et al. *A Near-infrared Study of the Highly-obscured Active Star-forming Region W51B J* *Korean Astron Soc.* **40** 17–28
- [47] Y. Hyodo et al. *Suzaku spectroscopy of extended X-ray emission in M17* *PASJ* **60** S85–S93